Journal of Electron Spectroscopy and Related Phenomena 226 (2018) 17–21

Contents lists available at ScienceDirect

Journal of Electron Spectroscopy and Related Phenomena

journal homepage: www.elsevier.com/locate/elspec

Electronic and magnetic properties of the (001) surface of the CoNbMnSi Heusler alloy: First-principles calculations

Jabbar M. Khalaf Al-zyadi [a,*], Ammar A. Kadhim [a], Kai-Lun Yao [b,c]

[a] Department of Physics, College of Education for Pure Sciences, University of Basrah, Iraq
[b] School of Physics and Wuhan National High Magnetic Field Center, Huazhong University of Science and Technology, Wuhan 430074, China
[c] International Center of Materials Physics, Chinese Academy of sciences, Shenyang, 110015, China

ARTICLE INFO

Article history:
Received 16 February 2018
Received in revised form 19 April 2018
Accepted 21 April 2018
Available online 23 April 2018

Keywords:
CoNbMnSi quaternary-Heusler alloy
Half-metallicity
Surface properties
First-principle study

ABSTRACT

In this paper, using first-principles calculations based on density-functional theory, the electronic structures, magnetic properties, and half-metallicity in the bulk and (001) surface of quaternary Heusler alloy CoNbMnSi are studied. For the bulk, the CoNbMnSi compound shows half-metallicity with a band gap of 0.5 eV in the down-spin direction at a equilibrium lattice constant of 5.88 Å. At a similar equilibrium lattice constant, the half-metallicity confirmed in the bulk CoNbMnSi, is ruined at both NbSi- and MnCo-terminated (001) surfaces and subsurfaces. Based on the magnetic property calculations, the magnetic moments of Mn and Nb atoms at the (001) surfaces increase with respect to the corresponding bulk values, while the magnetic moment of Co and Si atoms decreases. The spin-polarization ratio clearly decreases below 75% for (001) surfaces and subsurfaces of the CoNbMnSi alloy.

1. Introduction

The effective spin injection from a ferromagnet to a semiconductor is very essential for the improvement of the performance of spintronic devices [1], and thus materials with high Curie temperature, high spin polarization, and a compatible lattice structure with conventional semiconductors are required for application as a spintronic material. Half-metallic (HM) ferromagnets [2] demonstrate total (100%) spin polarization at Fermi level because the electronic structure is metallic in only one of the two spin channels. They are seen as the promising candidates as spin injection materials. Consequently, more and more HM ferromagnets with multiple structures have been predicted theoretically by first-principles calculations or proved experimentally in the past 35 years [3–7]. The spin-polarization is 100% at the Fermi energy (E_F) in the HM materials. It reveals two demeanors at the same time, one as a semiconductor or insulator with an energy gap at the Fermi energy and the other as metallic following the spin channel. Research on HM ferromagnets is rapidly growing since its prediction for NiMnSb in 1983 by de Groot and his collaborators [6]. Many theoretical studies are seen in different classes of materials, like the full-Heusler alloy [7], perovskite [8], pyrite-type [9], spinel [10], rutile-type [11], and certain transition metal pnictides and chalcogenides in zinc blende structure [12,13].

The $L2_1$ Heusler phase (space group 225, *Fm3m*) contains four interpenetrating face center cubic (fcc) lattices. If disparate atoms occupy each of the sublattices a quaternary Heusler structure is gained with an alternative symmetry, which is the renowned LiMgPdSn or Y-type structure (space group 216, *F43m*) [14,15]. Heusler compounds can illustrate tunable electronic and magnetic characteristics based on their valence electron count, so this group of materials offer a greater variety of possibilities for the design of rational materials. An important example is the quaternary alloy CoFeMnSi, which has an expected HM band structure [16]. More theoretical works on quaternary Heusler compounds CoFeCrZ conducted and experimented by Gao et al. [17] exposed that among all alloys detected, both CoFeCrAl and CoFeCrSi are excellent HM ferromagnets with huge HM gaps. They also revealed that the half-metalicity is ruined for CoFeCrAl and CoFeCrGa when the Coulomb interaction is regarded. At present, the limit of the half metals of a Heusler structure has been expanded to the compounds composing and including 4d elements [18–20], especially Co-based Heusler compounds. Co_2MnSi and Co_2FeSi compounds with a Hg_2CuTi type Heusler structure have been proved to be half metals based on first principles calculations, which have overtly enriched the potential implementation of Heusler alloys. Also, the quaternary Heusler alloys CoZrMnSi, CoTcMnSi, CoRhMnSi, CoFeCrSi, CoZrFeSi, and CoNbFeSi have been affirmed to be half metals. Among these quaternary Heusler alloys mentioned earlier, CoAgMnSi, CoMoMnSi,

* Corresponding author.
E-mail address: jabbar.khalaf@uobasrah.edu.iq (J.M.K. Al-zyadi).

https://doi.org/10.1016/j.elspec.2018.04.005
0368-2048/

CoYMnSi, and CoPdMnSi alloys can even be considered as spin gapless semiconductors [21]. It has been shown that a few quaternary alloys containing 4d elements, such as CoRhMnGa and CoRhMnSn [22,23], have been tested experimentally, but a large part of the current research concentrates on theoretically predicting half metallic materials containing 4d elements. Very recently, Kundu et al. [24] found the HM ferromagnetism in many quaternary Heusler alloys such as CoX′MnSi (X′ = Y, Zr, Nb, ...), only CoRuFeSi [25] has been experimentally synthesized based on some ternary Heusler alloys.

Theoretical or experimental studies on the thin films or multilayers of CoNbMnSi have never been carried out. These characteristics are highly significant to the practical spintronic applications, since the half metallicity of bulk may be lost at the surfaces and interfaces [26–28]. For example, previous studies showed that the half-metallicity verified in the bulk Mn_2CoSn is destroyed at (001) surfaces [29]. Furthermore, the half-metallicity of Mn_2CoAl (001) surface [30] was investigated via first-principles calculations. It has been shown that because of the strong surface's potential effect on the surface of Co atom, the CoMn-terminated (001) surface fails to preserve the half-metallicity, which can be seen and observed in the bulk.

In this paper, a first-principles study of the structural, electronic and magnetic properties of the bulk and (001) surface of quaternary Heusler compound CoNbMnSi has been presented. It is indicated that the bulk HM property is destroyed at the MnCo- and NbSi-terminated (001) surfaces for CoNbMnSi. In addition, the magnetic moments and spin polarizations are also discussed. Taking into account larger two dimensional unit cells at the surface (not considered here) could allow for other reconstructions patterns to occur.

2. Computational method

To explore the electronic and magnetic properties of the bulk and (001) surface of quaternary Heusler compound CoNbMnSi, we employ the first-principle full-potential linearized augmented plane-wave (FPLAPW) method implemented in the Wien2k code [31]. The functional electronic exchange correlation can be obtained within the generalized gradient approximation in the scheme of Perdew, Burke, and Enzerhof [32]. The k meshes of $12 \times 12 \times 12$ for the bulk and the use of the $12 \times 12 \times 1$ k meshes for the (001) surface in the Brillouin zone is selected. We restrict the number of plane waves by $R_{mt} \times K = 8$ and the expansion is made up to $l = 10$ in the muffin tins. In the present calculations, both in the bulk and surface systems, the muffin-tin radii are set to 2.3 a.u. for the transition metals besides the main group elements. The achievement of the self-consistency calculations can be considered when the total energy disparity between succeeding iterations is less than 13.6×10^{-5} eV per formula unit. The crystal structure of the quaternary Heusler alloy CoNbMnSi is known to be a highly ordered Hg_2CuTi-type structure. The type of atom arrangements in the quaternary Heusler compound are X_1X_2YZ: X_1 (1/4, 1/4,1/4), X_2 (1/2, 1/2, 1/2), Y (3/4, 3/4, 3/4), and Z (0, 0,0).

3. Results and discussion

3.1. Electronic structure of bulk CoNbMnSi

We consider the structural type of Hg_2CuTi for the quaternary Heusler compound CoNbMnSi. To determine the theoretical lattice constant, we present the calculated total energies as a function of the lattice constants by using the ferromagnetic calculations, as explained in Fig. 1. From the minimum value of the total energy, we obtained the equilibrium lattice constant. Our calculated equilibrium lattice constant of Hg_2CuTi-CoNbMnSi is 5.88 Å. It is applied

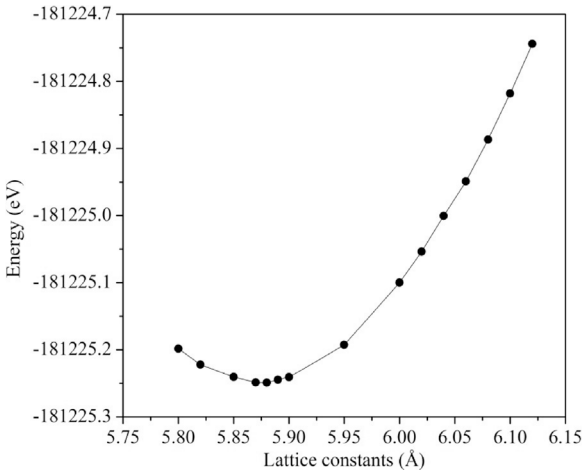

Fig. 1. The total energy as a function of lattice constant for CoNbMnSi in the Hg_2CuTi structure.

to our calculations and is approximately the same as the theoretical value of 5.85 Å [24], and the corresponding total energy is -181225.24906 eV.

The electronic band structure of the CoNbMnSi alloy in the irreducible Brillouin zone is exhibited in Fig. 2. The band structure of the quaternary Heusler compound CoNbMnSi shows a metallic behavior, because the majority spin (spin-up) electrons cross the Fermi level. In addition, there is an energy gap at the Fermi level in the minority (spin-down) channel. It means that the quaternary Heusler alloy CoNbMnSi is an HM ferromagnet. The HM is found to be weak, because the spin-down valence bands cross the energy level slightly. The energy gap in the spin-down channel is about 0.5 eV. Additionally, the HM gap is 0.237 eV (the HM gap, which is determined as the minimal between the lowest energy of down (up)-spin conduction bands with respect to the Fermi level and the absolute values of the top energy of down (up)-spin valence bands). The HM gap is a significant parameter in the spintronics and other implementations.

More significantly, the total magnetic moment per formula unit is an integer value because the integer value is a very meaningful condition for the quaternary Heusler alloy CoNbMnSi to be a HM ferromagnet. The total spin magnetic moment of CoNbMnSi comprises five sections: the spin magnetic moment of the Co atom ($0.800\mu_B$), the spin magnetic moment of the Nb atom $_B$), and the magnetic moment of interstitial area ($-0.055\mu_B$). Firstly, it means that the total spin magnetic moment is 1.00 μ_B per formula unit. Secondly, the main contribution to the total spin magnetic moment of CoNbMnSi comes from the 3d electrons in the Co atom. The calculated total spin magnetic moment complies with the Slater-Paulig behavior [33–35].

$$M_{tot} = (Z_{tot} - 24)\,\mu_B \quad (1)$$

Here M_{tot} is the total spin magnetic moment per formula unit and Z_{tot} is the total number of valence electrons in CoNbMnSi. Depending on electron configuration Co ($3d^7$, $4s^2$), Nb ($4d^4$, $5s^1$), Mn ($3d^5$, $4s^2$), and Si ($3s^2$, $3p^2$) have nine, five, seven, and four valence electrons, respectively. As a result, the total number of valence electrons is 25, which means that the total spin magnetic moment is 1 μ_B.

Fig. 3 shows the calculated total and partial density of states of CoNbMnSi, Co 3d, Nb 3d, Mn 3d, and Si 4p electrons. CoNbMnSi is an HM ferromagnet; accordingly, there is an energy gap in the minority-spin channel at the Fermi level, while the majority-spin electrons indicate metallic property, as shown in Fig. 3. The spinning minorities are factored by -1, and the Fermi levels are set to zero.

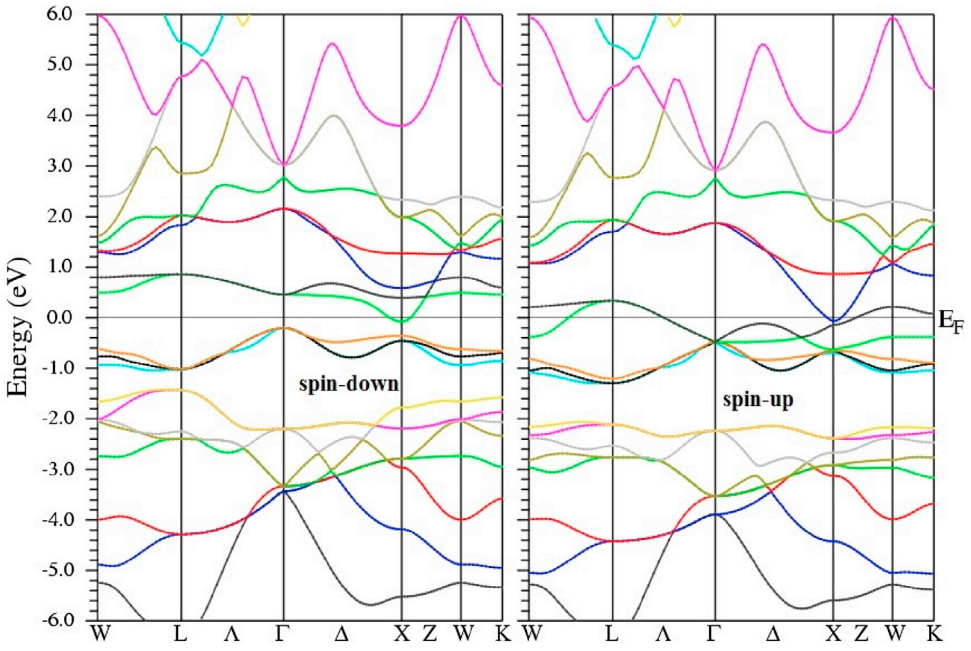

Fig. 2. The spin- down (left panel) and spin-up (right panel) band structures of bulk CoNbMnSi.

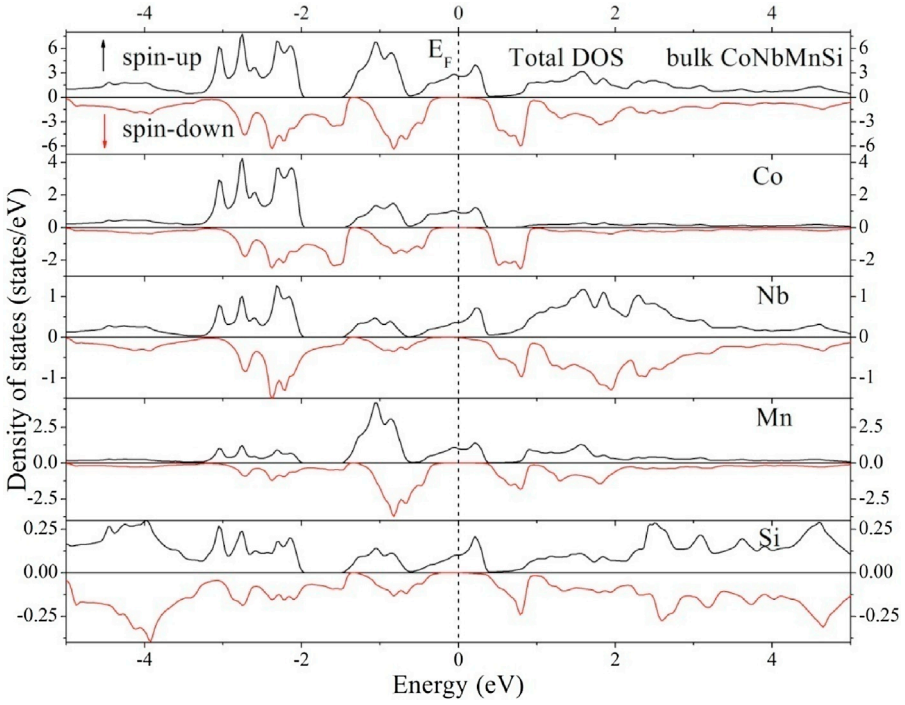

Fig. 3. The calculated total and partial densities of states of the quaternary Heusler alloy CoNbMnSi. The zero energy value corresponds to the Fermi level E_F.

From Fig. 3, one can see the main contribution to the total density of state of CoNbMnSi in the Hg_2CuTi structure that comes from the 3d electron (Co, Nb and Mn atoms) in the transition metals, and the contribution of p electron (Si atom) is very small.

3.2. Surface properties

For the practical implementation in spin electronic devices, the HM materials are commonly simulated to a thin film. However, the electronic characteristics of surface usually vary from that of the bulk. The surface is able to reduce the spin-polarization value and ruin the half-metallicity. So, the discussion of the surface influence on half-metallicity is very significant. The (001) surface of Hg_2CuTi-CoNbMnSi includes rotating atomic layers which comprise two kinds of terminations, which are named as a MnCo- and NbSi-terminated (001) surfaces. The slab containing thirteen monolayers of atom and a 15Å vacuum located above the surfaces in order to avert the interactions of sequential slabs. To shape an epitaxial thin film, nine internal atomic layers are fixed as the slabs and the top four atomic layers of the slabs are allowed to relax by minimizing the total energy and the atomic forces. Therefore, we get the equilibrium surface structure for both termination kinds.

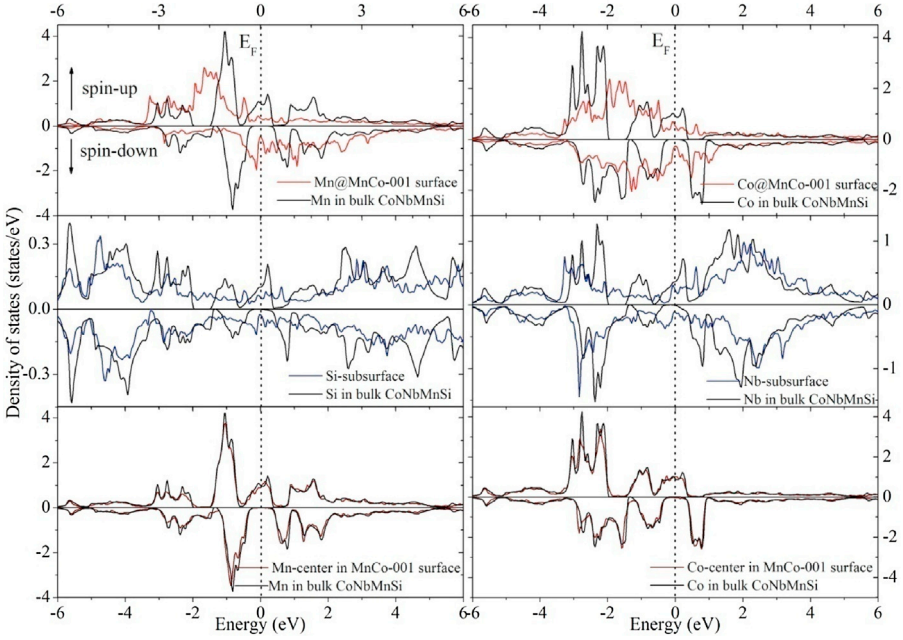

Fig. 4. Surface, subsurface, and middle-layers DOS of the CoNbMnSi (001) slab terminated with MnCo (red line). For comparison, the atomic-resolved DOS of Mn and Co atoms in bulk CoNbMnSi are also offered (black line) (For interpretation of the references to colour in this figure legend, the reader is referred to the web version of this article).

Moreover, we employ the equilibrium lattice constant of the bulk illustrated in Fig. 1 to construct the slab. The number of relaxed layers and the slab layers are sufficient to investigate the surface properties [23]. As such, the changes of magnetic moment and bond length of the surface are very small when vacuums and thicker slabs are used. The differences are less than 0.001 μ_B for the magnetic moment, and less than 0.002 Å for the bond length of surface atoms. Currently, we investigate the electronic structure, magnetic properties, spin-polarization and half-metallicity depending on the terminated (001) surface for CoNbMnSi compound. In the case of MnCo-terminated (001) surface, before the relaxation the bond lengths are 2.598 Å. After relaxation, the Mn—Nb, Mn—Si, Co—Nb, and Co—Si bonds lengths are 2.439, 2.423, 2.406, and 2.390 Å, respectively. While, at the NbSi-terminated (001) surface, After relaxation, the Nb—Co, Nb—Mn, Si—Co and Si—Mn bonds lengths are 2.564, 2.532, 2.503, and 2.474 Å, respectively.

Further, the DOS of the terminated (001) surfaces as indicated in Figs. 4 and 5 is clearly different from the bulk as illustrated in the Fig. 3. In addition, the atom-resolved DOS at the center-layer of the slabs and in the CoNbMnSi bulk are given for comparison. Figs. 4 and 5 provide an evidence that for two slabs, terminated with MnCo- and NbSi, the middle-layer atoms have DOS that is nearly the same as those in the CoNbMnSi bulk. That is to say the physical properties of bulk are repossessed in the middle-layer of the two slabs. So, the slabs with thirteen atomic layers are fitting to be employed to investigate the characteristics of the surfaces. Unfortunately, the DOS of Mn and Co atoms at the MnCo-terminated (001) surface and Nb and Si atoms at the NbSi-terminated (001) surface indicate that the spin-up and spin-down electrons have metallic properties. This means that the bulk half-metallicity of CoNbMnSi is ruined at the MnCo- and NbSi-terminated (001) surfaces because of the emergence of surface states inside the gap of the spin-down direction (see Figs. 4, 5). Matching the partial surface DOS with those in the bulk CoNbMnSi indicates that the MnCo- and NbSi-terminated (001) surfaces, spin-down and spin-up DOS move towards the low energy and away from the Fermi energy.

The calculated spin magnetic moments and spin polarization values of Mn, Co, Nb, and Si atoms on the surfaces, subsurfaces and middle layers of the slabs are exhibited in Table 1. For comparison, the analogical bulk magnetic moments values give a further evidence as clear in this table. Furthermore, we also observe that the spin magnetic moments values at the middle layer of the (001) surfaces are similar to those of the CoNbMnSi bulk, a matter that explains why the physical features of bulk are repossessed at the middle of the slabs. These results are a good confirmation of the suitable thickness of the slabs used to investigation the surface properties. Depending on the calculated magnetic moments values of surface atoms (see Table 1), it is clear that the magnetic moments values of surface atoms are 2.557 and 0.646 μ_B for Mn and Co atoms at the MnCo-terminated surface. In contrast, the magnetic moments values of Nb and Si atoms are −0.011 and −0.006 μ_B at the NbSi-terminated surface. The magnetic moment value of Mn and the absolute magnetic moment value of Nb are larger than those in the bulk system because the Mn and Nb atoms at the surfaces lose the electronic charge towards the vacuum. The magnetic moment value of Co and the absolute magnetic moment value of

Table 1
Magnetic moments (in unit of μ_B) for each atom in the bulk, surface (S), subsurface (subS) and middle (M) layers of the CoMnNbSi quaternary Heusler alloy. The calculations of spin polarization values (P) for the atoms are also demonstrated.

	Atom	M(μ_B)	P (%)
Bulk	Co	0.800	100%
	Mn	0.273	100%
	Nb	−0.010	100%
	Si	−0.008	100%
MnCo-ter	Mn (S)	2.557	12.39%
	Co (S)	0.646	34.92%
	Si (subS)	−0.031	37.24%
	Nb (subS)	−0.268	37.33%
	Mn (M)	0.271	100%
	Co (M)	0.816	100%
NbSi-ter	Nb (S)	−0.014	58.28%
	Si (S)	−0.006	74.05%
	Mn (subS)	0.789	73.61%
	Co (subS)	0.919	78.39%
	Nb (M)	−0.013	100%
	Si (M)	−0.008	100%

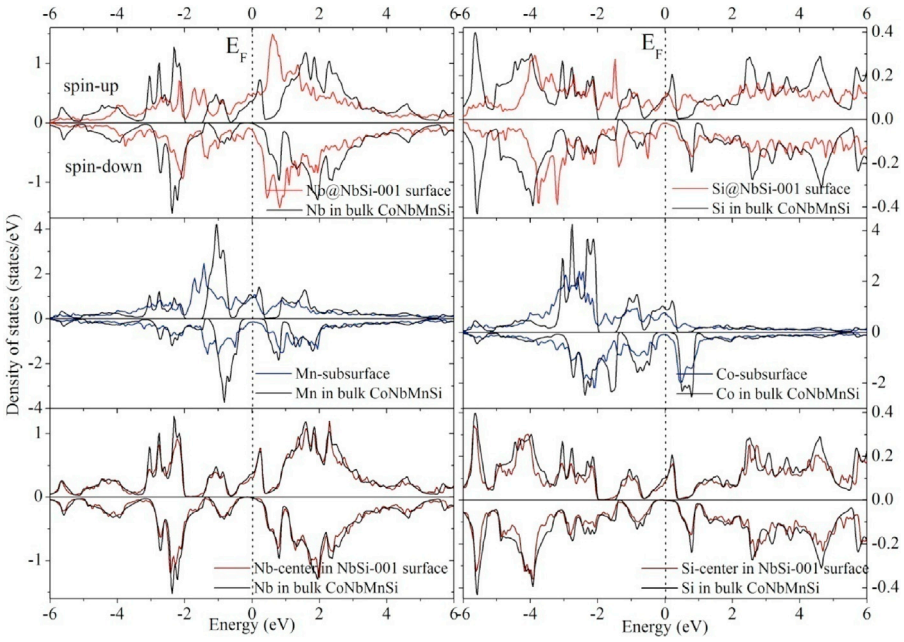

Fig. 5. Surface, subsurface, and center-layer DOS of the CoNbMnSi (001) slab terminated with NbSi (red line). For comparison, the DOS of Nb and Si atoms in bulk CoNbMnSi are also showed (black line) (For interpretation of the references to colour in this figure legend, the reader is referred to the web version of this article).

Si atom are smaller than those in the bulk system because of the decrease and increase of the electronic charge in the up and down spin channels, respectively. Contrarily, the magnetic moments values of the atoms at the subsurfaces increase greatly compared to the bulk values.

Depending on the identification of spin polarization $P = (N\uparrow - N\downarrow) / (N\uparrow + N\downarrow)$, where $N\uparrow$ is the DOS for the spin-majority and $N\downarrow$ is the DOS for the spin-minority channels at the Fermi energy, we also evaluate the spin polarization (see Table 1). As a result, the high spin polarized alloy is associated with the applications of spin electronic devices. The calculated spin polarizations of the terminated surface structures of the quaternary Heusler alloy CoMnNbSi are lower due to the ruined half-metallicity at the MnCo-terminated (001) surface. Though the (001) surface does not have a spin polarization of 100%, it has a high spin polarization (58.28% and 74.05% for surface atoms Nb and Si, respectively), which is compatible with the above results where the surface structure shows approximate HM properties (see Fig. 4).

4. Conclusion and summary

In summary, the first-principles FPLAPW method was performed to investigate the electronic structure, the magnetic properties and the half-metallicity of quaternary Heusler compound CoNbMnSi. This compound is predicted to be a half-metallic material with a band gap of 0.5 eV with an equilibrium lattice constant is 5.88 Å, and a spin magnetic moment of 1.00 μ_B per formula unit. The optimized equilibrium lattice constant is in good agreement with other theoretical results. The total magnetic moment is satisfied with the Slater-Pauling formula. For CoNbMnSi (001) surfaces, the half-metallicity is ruined and the spin-polarization ratio clearly decreases on all the terminated (001) surfaces for CoNbMnSi alloy. The calculations further explain that the spin magnetic moments of Mn and Nb atoms in the bulk are 0.273 and −0.010 μ_B and then increase to 2.557 and −0.014 μ_B at the surfaces, respectively. But the spin magnetic moments of Co and Si atoms in the bulk are 0.800 and −0.008 μ_B and decrease to 0.646 and −0.006 μ_B at the surfaces, respectively.

References

[1] I. Zutic, J. Fabian, S. Das Sarma, Rev. Mod. Phys. 76 (2004) 323.
[2] R.A. de Groot, F.M. Mueller, P.G. van Engen, K.H.J. Buschow, Phys. Rev. Lett. 50 (1983) 2024.
[3] M.I. Katsnelson, V.Yu. Irkhin, L. Chioncel, A.I. Lichtenstein, R.A. de Groot, Rev. Mod. Phys. 80 (2008) 315.
[4] C. Felser, G.H. Fecher, B. Balke, Angew. Chem. Int. Ed. 46 (2007) 668.
[5] K.H.J. Buschow, P.G. van Engern, J. Magn. Magn. Mater. 25 (1981) 90.
[6] R.Y. Umetsu, K. Kobayashi, R. Kainuma, Y. Yamaguchi, K. Ohoyama, A. Sakuma, K. Ishida, J. Alloys Comp. 499 (2010) 1.
[7] G.Y. Gao, K.L. Yao, J. Appl. Phys. 111 (2012) 11370.
[8] J.H. Park, E. Vescovo, H.J. Kim, C. Kwon, R. Ramesh, T. Venkatesan, Nature 392 (1998) 794.
[9] T. Shishidou, A.J. Freeman, R. Asahi, Phys. Rev. B 64 (2001) 180401.
[10] F.J. Jedema, A.T. Filip, B.J. van Wees, Nature 410 (2001) 345.
[11] Y. Ji, G.J. Strijkers, F.Y. Yang, C.L. Chien, J.M. Byers, A. Anguelouch, G. Xiao, A. Gupta, Phys. Rev. Lett. 86 (2001) 5585.
[12] H. Akinaga, T. Manago, M. Shirai, Jpn. J. Appl. Phys. 39 (Part 2) (2000) L1118.
[13] M.G. Sreenivasan, J.F. Bi, K.L. Teo, T. Liew, J. Appl. Phys. 103 (2008) 043908.
[14] U. Eberz, W. Seelentag, H.U. Schuster, Z. Naturforsch. B 35 (1980) 1341.
[15] H. Pauly, A. Weiss, H. Witte, Z. Metallkunde 59 (1968) 47.
[16] X. Dai, G. Liu, G.H. Fecher, C. Felser, Y. Li, H. Liu, J. Appl. Phys. 105 (2009) 07E.
[17] G.Y. Gao, Lei Hu, K.L. Yao, Bo Luo, Na Liu, J. Alloy. Compd. 551 (2013) 539.
[18] X.T. Wang, X.F. Dai, L.Y. Wang, X.F. Liu, W.H. Wang, G.H. Wu, C.C. Tang, G.D. Liu, J. Magn. Magn. Mater. 378 (2015) 16.
[19] Z.Y. Deng, J.M. Zhang, J. Magn. Magn. Mater. 397 (2016) 120.
[20] H.H. Xie, Q. Gao, L. Li, G.Lei.G.Y. Mao, X.R. Hu, J.B. Deng, Comput. Mater. Sci. 103 (2015) 52.
[21] X.L. Wang, Phys. Rev. Lett. 100 (2008) 156404.
[22] V. Alijani, J. Winterlik, G.H. Fecher, S.S. Naghavi, S. Chadov, T. Gruhn, C. Felser, J. Phys. Condens. Mat. 24 (2012) 4.
[23] M. Benkabou, H. Rached, A. Abdellaoui, D. Rached, R. Khenata, M.H. Elahmar, B. Abidri, N. Benkhettou, S. Bin Omran, J. Alloy. Compd. 647 (2015) 276.
[24] A. Kundu, S. Ghosh, R. Banerjee, S. Ghosh, B. Sanyal, Sci. Rep. 7 (2017) 1803.
[25] Lakhan Bainsla, M.M. Raja, A.K. Nigam, K.G. Suresh, J. Alloy. Compd. 651 (2015) 631.
[26] J.M. Khalaf Al-zyadi, G.Y. Gao, K.L. Yao, Solid State Commun. 152 (2012) 1244.
[27] J.M. Khalaf Al-zyadi, G.Y. Gao, K.L. Yao, J. Magn. Magn. Mater. 378 (2015) 1.
[28] J.M. Khalaf Al-zyadi, M.H. Jolan, K.L. Yao, J. Magn. Magn. Mater. 403 (2016) 8.
[29] J.M. Khalaf Al-zyadi, G.Y. Gao, K.L. Yao, J. Alloy. Compd. 565 (2013) 17.
[30] J. Li, Y. Jin, Appl. Surf. Sci. 283 (2013) 876.
[31] P. Blaha, K. Schwarz, G.K.H. Madsen, D. Kvasnicka, J. Luitz, Wien2k, Vienna University of Technology, 2002. improved and updated Unix version of the original copyrighted Wiencode, which was published by P. Blaha, K. Schwarz, P. Sorantin, S.B. Trickey, Comput. Phys. Commun. 59 (1990) 399.
[32] J.P. Perdew, K. Burke, M. Ernzerhof, Phys. Rev. Lett. 77 (1996) 3865.
[33] I. Galanakis, P.H. Dederichs, N. Papanilolaou, Phys. Rev. B 66 (2002) 174429.
[34] H.C. Kandpal, G.H. Fecher, C. Felser, J. Phys. D 40 (2007) 1507.
[35] T. Graf, C. Felsler, S.P.P. Parkin, Prog. Solid State Chem. 39 (2011) 1.